Environmental Science & Technology

ARTICLE

pubs.acs.org/est

Dissolved Organic Carbon Enhances the Mass Transfer of Hydrophobic Organic Compounds from Nonaqueous Phase Liquids (NAPLs) into the Aqueous Phase

Kilian E. C. Smith,*,† Martin Thullner, Lukas Y. Wick, and Hauke Harms

UFZ Helmholtz Centre for Environmental Research, Department of Environmental Microbiology, Leipzig, Germany

Supporting Information

ABSTRACT: The hypothesis that dissolved organic carbon (DOC) enhances the mass transfer of hydrophobic organic compounds from nonaqueous phase liquids (NAPLs) into the aqueous phase above that attributable to dissolved molecular diffusion alone was tested. In controlled experiments, mass transfer rates of five NAPL-phase PAHs (log K_{OW} 4.15−5.39) into the aqueous phase containing different concentrations of DOC were measured. Mass transfer rates were increased by up to a factor of 4 in the presence of DOC, with the greatest enhancement being observed for more hydrophobic compounds and highest DOC concentrations. These increases could not be explained by dissolved molecular diffusion alone, and point to a parallel DOC-mediated diffusive pathway. The nature of the DOC-mediated diffusion pathway as a function of the DOC concentration and PAH sorption behavior to the DOC was investigated using diffusion-based models. The DOC-enhanced mass transfer of NAPL-phase hydrophobic compounds into the aqueous phase has important implications for their bioremediation as well as bioconcentration and toxicity.

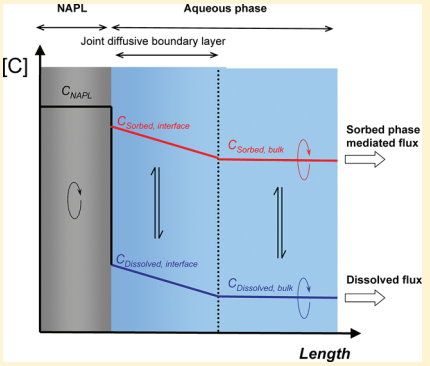

INTRODUCTION

Hydrophobic organic compounds (HOCs) are often found as mixtures in the form of nonaqueous phase liquids (NAPLs), such as hydrocarbon oil spills or industrial NAPLs contaminating terrestrial and aquatic environments. Due to their hydrophobic nature, the HOCs preferentially remain in the NAPL, with slow mass transfer into the aqueous phase.[1−3] Because water-dissolved HOCs play a key role in diffusive uptake into organisms,[4−6] this has contrasting implications for the biota inhabiting NAPL-contaminated environments. Microorganisms using HOCs as a source of carbon and energy face a large reservoir of inaccessible food in the NAPL, often reflected in slow bioremediation of NAPL contaminated sites.[7] However, HOC bioconcentration can also lead to toxicity.[8] Here, low aqueous concentrations and thus reduced bioconcentration might ameliorate detrimental effects of the NAPL pollution. In NAPL-polluted aquifers, mass transfer into the aqueous phase also determines groundwater contamination, with consequences for human health and the effectiveness of water-based remediation technologies.[7,9]

Often, process dynamics mean that equilibrium partitioning between the NAPL and aqueous compartments is not reached, and aqueous concentrations are determined by mass exchange kinetics.[10,11] Therefore, to understand NAPL toxicity and (bio)remediation, evaluation of the key controlling factors is required. There are many influences on NAPL to aqueous phase mass transport, including mixing[10] and interfacial area,[9] NAPL viscosity and surface film development,[3,12] and the properties of the component HOCs.[1,2] Furthermore, biodegrading organisms can lead to altered mass fluxes. Microbial adaptations such as biofilm formation,[13] chemotaxis,[14] or surfactant production,[15] can increase mass fluxes compared to abiotic dissolution alone. Biofilms can also provide an additional diffusive barrier reducing mass transfer.[16]

Mobile "colloid-like" phases can contribute to diffusive mass exchange processes between surfaces and the bulk aqueous phase,[17−18] a phenomenon termed enhanced or facilitated diffusion. For example, surfactants micelles can increase, decrease, or negligibly impact mass transfer from NAPLs into the aqueous phase depending on the surfactant, NAPL properties and architecture, and pore-water flow.[20−22] Enhanced diffusion has also been studied in the context of other HOC exchange fluxes, including polymer−water exchange,[23−26] aquatic bioaccumulation,[27] and biodegradation.[28] The nature of the sorbing phases leading to enhanced diffusion is varied, including nanoparticles,[23] proteins,[26] and dissolved organic carbon (DOC).[24,25,27,28] The ubiquity of DOC and its propensity to sorb HOCs raises the relevant question as to whether DOC can increase mass transfer of HOCs out of a NAPL and into the surrounding aqueous phase, and what the implications are for biodegradation and toxicity. The important role of DOC in enhancing metal mass fluxes and availability to organisms is well recognized, and the theoretical basis describing the relevant processes exists.[19,18,29,30]

Received: January 23, 2011
Accepted: August 31, 2011
Published: August 31, 2011

This study was conceived to test the hypothesis that DOC increases mass fluxes of HOCs from a NAPL into the aqueous phase above those attributable to dissolved diffusion alone. As representative HOCs, five PAHs (log K_{OW} 4.15−5.39) were dissolved in 2,2,4,4,6,8,8-heptamethylnonane (HMN) as a model NAPL. PAH mass transfer into saline aqueous medium containing different concentrations of DOC were measured over time using equilibrium negligible depletion-solid phase microextraction (nd-SPME). This study was part of a larger effort looking at contamination in the marine environment, hence the use of saline medium. The temporal development in dissolved and DOC-sorbed PAH concentrations were interpreted using diffusion models, accounting for any contribution of DOC-enhanced diffusion.

MATERIALS AND METHODS

The complete experimental section is given in the Supporting Information (SI) and only a summary is provided below.

Experimental Setup. Mass transfer experiments were carried out in the setup shown in Figure S1 with 2 L of saline medium (see Table S1) containing 0, 0.0226, or 0.226 g DOC L^{-1}. The glass tube (250 mm long, 25 mm id) was inserted through the lid to 3 cm below the water surface and experiments started by adding 1 mL of HMN containing PAHs, each at approximately 1 g L^{-1} (see Table S2), to the inside of the glass tube so that it floated on the surface of the water to give a defined and constant surface area. The bottles were kept at 22 °C under stirring conditions sufficient to keep the aqueous phase homogeneous, while avoiding breaking of the NAPL/water interface. For each DOC concentration, duplicate experiments were conducted on different dates.

Sampling and nd-SPME Analysis. Equilibrium nd-SPME with internal standards was used to measure the total, DOC-sorbed, and dissolved aqueous PAH concentrations.[28,31] At intervals (see Table S3), 10-mL aqueous samples were taken and deuterated PAHs were added as internal standards together with a 0.5-cm length of polydimethylsiloxane (PDMS)-coated SPME fiber. These were shaken for 24 h to allow equilibrium to be reached (see Figure S2), before placing the fibers in 100 μL of toluene containing 1 μg of acenaphthylene-d_8 as an injection standard to re-extract the PDMS sorbed PAHs.

Total, DOC-Sorbed and Dissolved PAH Concentrations. Dissolved concentrations in the DOC samples were calculated using a 4-point external calibration performed in triplicate (n = 12). PAH concentrations in the PDMS were plotted against those in the saline medium (Figure S3), with the slopes giving the PDMS: saline medium partitioning ratios $K_{PDMS/d}$ (L L^{-1}) (Table S4) for converting the PDMS sorbed PAH concentrations into dissolved concentrations. Quantifying the PDMS sorbed PAHs relative to the PDMS sorbed PAH internal standards gives the total aqueous concentrations, and does not require calibration of the SPME method.[31] In the experiments with saline medium, total concentrations are equivalent to the dissolved concentrations. In experiments with DOC, these represent the dissolved plus sorbed concentrations. DOC-sorbed concentrations are calculated by difference, without the necessity of assuming a complete mass balance.

HMN Concentrations. The initial concentrations of PAHs in the HMN were analyzed by dissolving 50 μL of the HMN in 950 μL of toluene and adding 1 μg of each deuterated PAH in toluene as internal standards.

Analysis and Quantification. GC-MS analyses were performed using an HP 6890 Series GC (Hewlett-Packard, California, USA), with a 30-m HP5MS capillary column (0.25 mm i.d. and 0.25 μm film thickness) and 2 m uncoated and deactivated HP retention gap (0.53 mm i.d.) in selected ion monitoring mode (SIM). PAHs were quantified using the HP Environmental Data Analysis software. Before adding the HMN containing the PAHs to start an experiment, a medium sample was taken from each setup as a blank. These blanks amounted to less than 2% of the final concentrations, and were subtracted from the aqueous concentrations measured during the experiments. Data were fitted by the least-squares method using Graphpad Prizm 5 (San Diego, CA, USA), giving the respective rate constants and equilibrium concentrations.

Fitting the Data and Modeling of Enhanced Diffusion. A complete description of the modeling approaches is given in the SI, with only a summary given below.

Mass transfer of PAHs from the NAPL into the aqueous compartment leads to an increase in the total concentration c_{tot} (μg L^{-1}) with time t (h). In the presence of DOC, c_{tot} is given as the sum of dissolved c_d (μg L^{-1}) and DOC sorbed c_s (μg L^{-1}) concentrations

$$c_{tot} = c_d + c_s = c_d + [DOC]\cdot K_{DOC/d}\cdot c_d = c_d\cdot(1 + [DOC]\cdot K_{DOC/d}) \quad (1)$$

where [DOC] (kg DOC L^{-1}) is the aqueous concentration of the DOC and $K_{DOC/d}$ (L kg DOC $^{-1}$) is the partitioning ratio between DOC sorbed and the dissolved phases. In the absence of DOC, c_{tot} is equal to c_d, and the rate of change in aqueous concentration $\partial c_{tot}/\partial t = \partial c_d/\partial t$ (μg L^{-1} h^{-1}) can be described using the two-film model[2]

$$c_d(t) = c_{eq,d}\cdot(1 - \exp(-k_d\cdot t)) \quad (2)$$

where k_d (h^{-1}) is the mass transfer rate constant and $c_{eq,d}$ (μg L^{-1}) is the dissolved concentration in equilibrium with the NAPL phase. Fitting eq 2 to the measured $c_d(t)$ allows $c_{eq,d}$ and k_d to be determined.

The dominant resistance to the mass transfer lies in the aqueous phase,[2] and k_d is determined by diffusion within an aqueous diffusive boundary layer (BL). Provided the NAPL surface area, aqueous volume, and mixing remain constant, $c_{eq,d}$ and k_d is given by

$$k_d = \frac{A}{V}\cdot m_d = \frac{A}{V}\cdot\frac{D_d}{\delta_d} \quad (3)$$

where A (equal to 4.91 × 10^{-4} m^2) is the NAPL/aqueous interfacial area, V (equal to 2 L) is the volume of the aqueous phase, m_d (m h^{-1}) is the mass transfer velocity, D_d (m^2 h^{-1}) is the molecular diffusion coefficient, and δ_d (m) is the thickness of the molecular diffusive BL of the PAH in question.

In the experiments with DOC, an equation analogous to eq 2 can be fitted to the measured $c_{tot}(t)$ to determine a compound mass transfer rate constant k_{tot} (h^{-1}).

$$c_{tot}(t) = c_{eq,tot}\cdot(1 - \exp(-k_{tot}\cdot t)) \quad (4)$$

where $c_{eq,tot}$ (μg L^{-1}) is the total aqueous concentration in equilibrium with the NAPL.

DOC might lead to two scenarios: (i) it does not influence dissolution, and molecular diffusion alone determines the changes in aqueous concentrations or (ii) DOC mediates an additional diffusive pathway across the BL. In the latter case, the diffusion of the dissolved and sorbed PAHs can be described by an average

diffusion coefficient $\overline{D}$ ($m^2\ h^{-1}$), weighted for the dissolved and sorbed fractions.[19,18]

$$\overline{D} = \frac{D_d + D_s \cdot \xi \cdot [DOC] \cdot K_{DOC}}{1 + [DOC] \cdot K_{DOC}} \quad (5)$$

where D_s ($m^2\ h^{-1}$) is the diffusion coefficient of the DOC-sorbed PAH and ξ (unitless) is a lability factor describing that portion of the sorbed PAH that can be considered labile. This ranges between 0 (completely nonlabile) and 1 (fully labile) (see SI for more details). The value of k_{tot} derived from fitting eq 4 to the experimental data can, analogously to eq 3, be defined in terms of $\overline{D}$ and $\overline{\delta}$,[32]

$$k_{tot} = \frac{A}{V} \cdot m_{tot} = \frac{A}{V} \cdot \frac{\overline{D}}{\overline{\delta}} \quad (6)$$

where m_{tot} ($m\ h^{-1}$) is the compound mass transfer velocity and $\overline{\delta}$ (m) is the thickness of the joint diffusive BL. The value of $\overline{\delta}$ is intermediate between δ_d and the thickness of the diffusive BL for the DOC-sorbed PAHs δ_s (m),[33] and can be calculated as described in the SI. By substituting eq 5 into eq 6, an expression for the compound mass transfer rate constant k_{tot} is obtained

$$k_{tot} = \frac{k_d^* + k_s^* \cdot \xi \cdot [DOC] \cdot K_{DOC/d}}{1 + [DOC] \cdot K_{DOC/d}} \quad (7)$$

where the mass transfer rate constants k_d^* ($= A/V \cdot D_d/\overline{\delta}$) and k_s^* ($= A/V \cdot D_s/\overline{\delta}$) are defined with respect to the thickness of the joint diffusion layer $\overline{\delta}$.

For the situation where DOC does not contribute to the diffusive transport, k_{tot} in eq 7 reduces to

$$k_{tot,\,dissolved} = \frac{k_d}{1 + [DOC] \cdot K_{DOC/d}} \quad (8)$$

where $k_{tot,dissolved}$ (h^{-1}) is the mass transfer rate constant when only dissolved molecular diffusion contributes to the process. All the parameters for calculating $k_{tot,dissolved}$ using eq 8 are independently measured. Fitting the PAH concentration profiles from the saline medium set-ups give k_d (defined in terms of D_d and δ_d), [DOC] is known, and $K_{DOC/d}$ is determined from the nd-SPME measurements. Therefore, when DOC does not play a role in the mass transfer process, values of k_{tot} derived from fitting eq 4 to $c_{tot}(t)$ should be identical to values $k_{tot,dissolved}$ calculated using eq 8. In the case of DOC-enhanced diffusion, fitted values of k_{tot} will be higher due to an additional contribution mediated by the DOC.

When DOC contributes to the diffusive transport k_{tot} is given by the full eq 7. Apart from the product $k_s^* \cdot \xi$, the parameters in eq 7 are independently known (D_d and D_s from the literature, $\overline{\delta}$ is calculated as described in the SI, [DOC] is known, and $K_{DOC/d}$ is measured). Therefore, the value of k_{tot} obtained from fitting eq 4 to $c_{tot}(t)$ allows eq 7 to be solved for $k_s^* \cdot \xi$. The product $k_s^* \cdot \xi$ contains information about the diffusion coefficient of the DOC-sorbed PAH, the thickness of $\overline{\delta}$, and the lability the sorbing DOC aggregates. For complete lability of the sorbed PAH this reduces to k_s^*.

RESULTS AND DISCUSSION

Are the Assumptions Behind the Modeling Approaches Met? The correct interpretation and comparison of the kinetic rate constants from the various experiments requires a homogeneous aqueous phase of constant volume, the HMN interface area and PAH concentrations are constant, and partitioning can be described by a single $K_{DOC/d}$ value. Mixing conditions were sufficiently vigorous to ensure a homogeneous aqueous phase (see duplicate experiment data in Figure S4). The cumulative volume removed was between 5 and 8% for the different experiments, and thus V can be taken as constant. The dissolved aqueous concentrations immediately adjacent to the HMN interface are assumed to be in instantaneous equilibrium with the HMN. These cannot be measured directly and are inferred from the bulk aqueous concentrations at system equilibrium. Significant depletion of the HMN due to mass transfer into the aqueous phase would render this approach invalid.[1] Maximum depletion of the HMN due to mass transfer into the aqueous phase was lower than 12%, with the exception of acenaphthene, fluorene, and phenanthrene in the highest DOC experiment where depletion was still less that 20% (Table S5). Therefore, the aqueous interface concentrations were taken as constant and equal to the bulk dissolved concentration at equilibrium. The validity of the assumption that PAH partitioning is well-described by a single $K_{DOC/d}$ value is shown in Figure S5, where sorbed PAH concentrations are plotted against C_d for the DOC 0.226 g L^{-1} experiments. In agreement with the literature for this DOC type,[34] sorption was linear over the range in experimental dissolved concentrations implying that the DOC concentration and sorbing properties remained unchanged. The total and dissolved concentrations measured using nd-SPME were used to calculate $K_{DOC/d}$ for both DOC concentrations, and the mean values are shown in Figure S6 and tabulated in Table S6. $K_{DOC/d}$ values increased with PAH hydrophobicity, falling within the range given in the literature.[34] For the less hydrophobic acenaphthene to phenanthrene, sorbed concentrations in the DOC 0.0226 g L^{-1} treatment were too low to allow $K_{DOC/d}$ to be reliably determined. $K_{DOC/d}$ values were slightly higher at DOC 0.226 g L^{-1} compared to the low DOC treatment by a factor of 1.9 and 3.6 for fluoranthene and pyrene, respectively. Because enhanced diffusion could only be discerned at the higher DOC concentration, the values from the DOC 0.226 g L^{-1} experiments have been used for the calculations below.

Mass Transfer into Saline Medium. Figure S4 shows the increase in saline medium PAH concentrations for the duplicate experiments over time. Good agreement attests to the reproducibility of the setup and measurement protocols. PAH dissolved concentrations increased before leveling out within the experiment duration as a partitioning equilibrium between the HMN and aqueous phases was reached. The values of $c_{eq,d}$ and k_d were obtained by fitting eq 2 to the $c_d(t)$ data, and are summarized in Table S7 together with the values of m_d and δ_d calculated using eq 3. $C_{eq,d}$ decreased with increasing PAH hydrophobicity because of the increased partitioning to the HMN. This is evident from Figure S7 where log $K_{HMN/d}$ for the different PAHs are plotted against log K_{OW}, increasing with PAH hydrophobicity (log $K_{HMN/d}$ = 0.772 log K_{OW} + 1.020; r^2 = 0.98). The fitted mass transfer rate constants k_d were similar for all PAHs, ranging by less than a factor of 1.5 from 0.0114 h^{-1} for pyrene to 0.0173 h^{-1} for fluorene (Figure 2). These are directly reflected in the values of m_d which varied between 4.66×10^{-2} m h^{-1} for pyrene to 7.03×10^{-2} m h^{-1} for fluorene. The δ_{BL} values ranged between 31 and 43 μm (Table S7), as expected given the identical hydrodynamic conditions and similarity in the molecular diffusion coefficients. Although the magnitudes of k_d (and therefore also m_d) and δ_{BL} are system dependent, similar trends between HOCs have also been observed in other studies.[2,35]

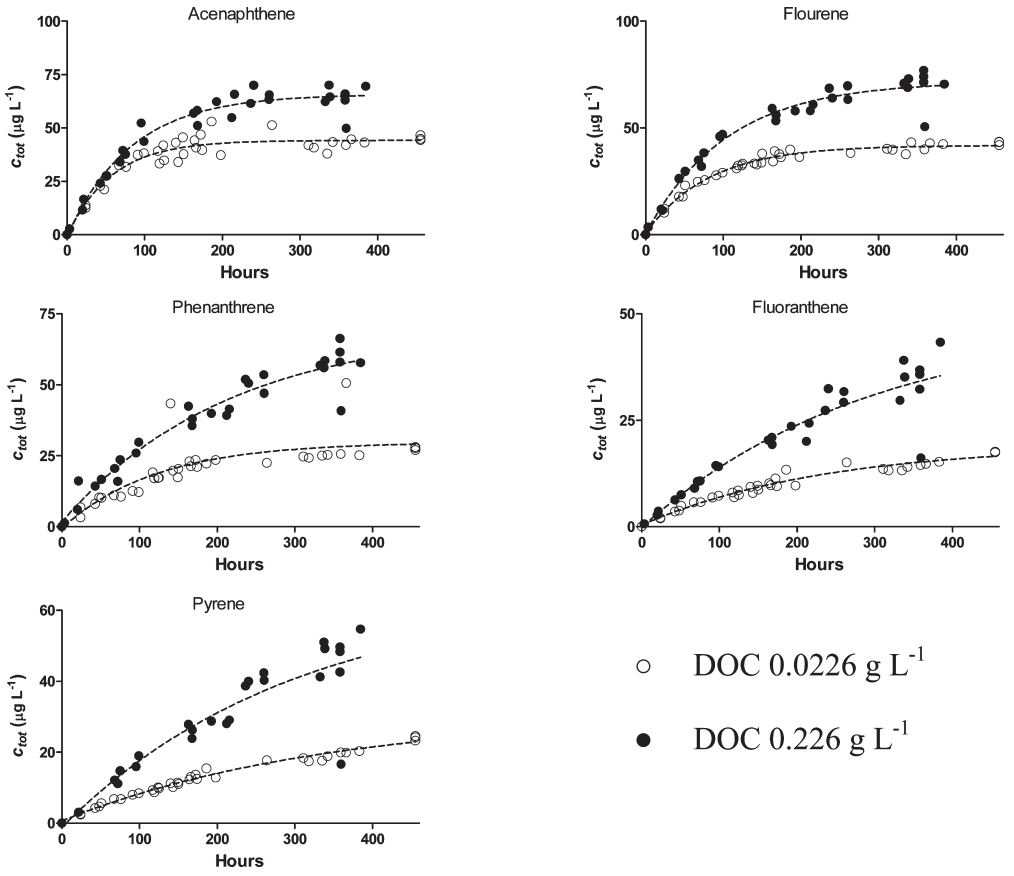

Figure 1. Mass transfer of PAHs in HMN into saline medium containing DOC concentrations of 0.0226 and 0.226 g L^{-1}. The dashed lines show the best fit of eq 4 to $c_{tot}(t)$.

Mass Transfer into Saline Medium with DOC. Figure 1 shows the temporal change in c_{tot} for the experiments with 0.0226 and 0.226 g DOC L^{-1} (Figure S8 shows c_{tot} and c_d). With increased sorption to the DOC, it takes longer for the system to attain partitioning equilibrium, and indeed for the heavier PAHs this was not reached within the duration of the experiment. The c_d values were similar to or lower than c_{tot} (Figure S8) with the difference increasing with either increasing PAH hydrophobicity and DOC concentration because of increased sorption. For acenaphthene to phenanthrene in the low 0.0226 g L^{-1} DOC treatment, there was a small positive bias in c_d, with these being higher than c_{tot} by a factor of up to 1.5. This might lie in either DOC altering the activity coefficient of the PAHs in the aqueous environment relative to that of the pure saline medium used for calibration,[36] or perhaps the manufacturer-supplied PDMS volume per unit length of fiber was too low for this batch of fibers. In the case of significant variations in coating thickness along the fiber length, the short lengths needed to avoid dissolved phase depletion may also have contributed. Important to note is that all rate parameters were determined from fitting the c_{tot} data, and c_d was used only to calculate $K_{DOC/d}$.

The $c_{tot}(t)$ data were fitted using eq 4 to obtain k_{tot}, with the values shown in Figure 2 (and tabulated in Table S8). The values of k_{tot} are generally lower than those of k_d, with the difference increasing with PAH hydrophobicity. For the DOC 0.0226 g L^{-1} experiments, k_{tot} ranged from 0.00295 h^{-1} for pyrene to 0.01750 h^{-1} for acenaphthene. For the DOC 0.226 g L^{-1} experiments, these were comparable, ranging from 0.00334 h^{-1} for pyrene to 0.01217 h^{-1} acenaphthene. For both DOC treatments, k_{tot} decreased with increasing PAH hydrophobicity.

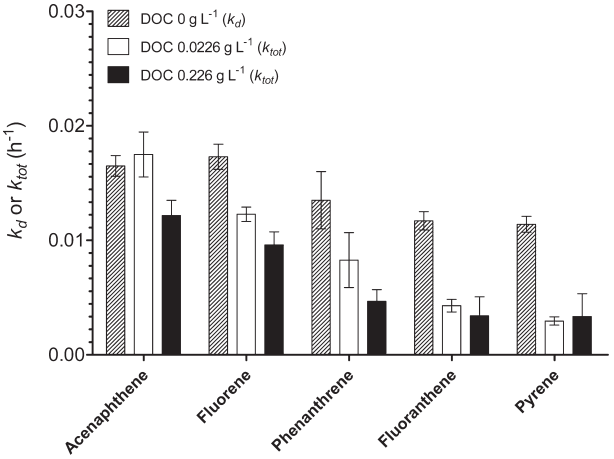

Figure 2. Dissolved (k_d, h^{-1}) and total (k_{tot}, h^{-1}) mass transfer rate constants together with their standard errors, obtained by fitting eqs 2 and 4 to $c_d(t)$ and $c_{tot}(t)$, respectively.

Contribution of DOC-Enhanced Diffusion. Figure 3 shows the ratio of k_{tot} (from fitting eq 4 to the measured $c_{tot}(t)$) to $k_{tot,dissolved}$ (calculated using eq 8) for both DOC concentrations. The calculated values of $k_{tot,dissolved}$ assume that DOC increases the capacity of the aqueous phase for the PAHs but does not

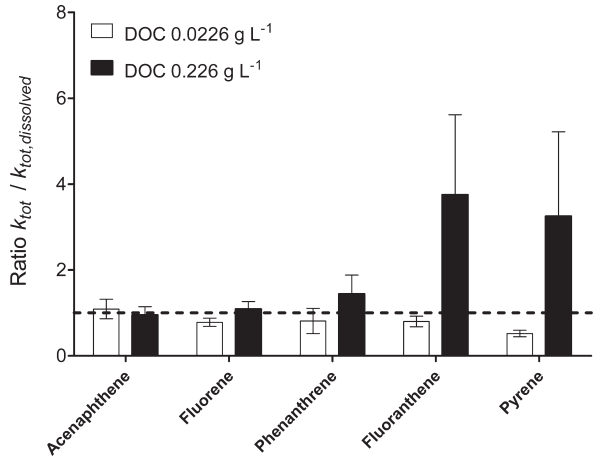

Figure 3. Ratio of k_{tot} (from fitting eq 4 to $c_{tot}(t)$) to $k_{tot,dissolved}$ (calculated using eq 8) for the low and high DOC treatments. The values of $k_{tot,dissolved}$ assume that DOC acts as a simple sorbing phase and does not mediate an additional diffusive flux. A ratio of $k_{tot}/k_{tot,dissolved}$ higher than one (indicated by the dashed line) implies that DOC-enhanced diffusion contributes to k_{tot}. Standard errors were calculated via error propagation.

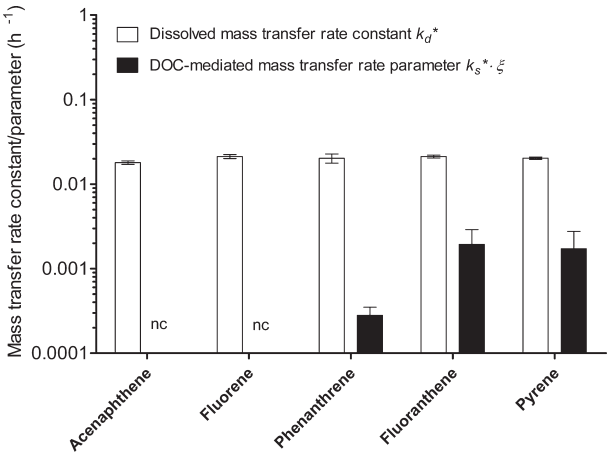

Figure 4. Dissolved (k_d*, h^{-1}) and DOC-mediated (k_s*·ξ, h^{-1}) mass transfer rate parameters for the DOC 0.226 g L^{-1} concentration. The standard errors of k_s*·ξ were calculated via error propagation. For acenapthene and fluorene, k_{tot} and k_d* overlapped and k_s*·ξ and could not be calculated (nc).

mediate an additional diffusive flux, such that k_{tot} is determined solely by k_d. Therefore, a $k_{tot}/k_{tot,dissolved}$ ratio higher than one implies an additional contribution to k_{tot} over and above that from k_d. For the lower DOC concentration, the $k_{tot}/k_{tot,dissolved}$ ratios for all PAHs are close to one, indicating that enhanced diffusion due to the DOC is not discernible under these conditions. For the higher DOC concentration experiments, the $k_{tot}/k_{tot,dissolved}$ ratios range from 0.99 for acenapthene up to 3.8 for fluoranthene. For the more hydrophobic PAHs the values higher than one imply that dissolved diffusion alone cannot explain the changes in c_{tot}, and that DOC-enhanced diffusion contributes to k_{tot}. Increases of a similar magnitude have been observed in other studies investigating DOC-enhanced diffusion of HOCs. For example, relative to the case with pure water, mass transfer rate constants measured for polymer exchange increased by a factor of up to 8 for these same PAHs in the presence of a DOC concentration of 0.383 g L^{-1}.[25]

Given the minimal effects of DOC at a concentration of 0.0226 g L^{-1}, the focus of the following discussion is on the data from the high DOC treatment. Equation 7 was used to calculate k_s*·ξ(tabulated in Table S8), with these shown in Figure 4 together with the values of k_d* calculated assuming D_s is 1 order of magnitude below D_d.[33,37] For acenapthene and fluorene, k_{tot} and k_d* overlapped and k_s*·ξ could not be calculated. Calculated values of k_s*·ξ were 0.00028, 0.00194, and 0.00172 for phenanthrene, fluoranthene, and pyrene, respectively.

The mass transfer rate constant for the DOC-mediated pathway k_s* contains the parameters A, V, D_s, and $\bar{\delta}$. These are known or can be calculated, and it is possible to independently arrive at a setup value for k_s*. Therefore, it should be possible to calculate ξ from the k_s*·ξ values in Table S8. Calculated values of ξ (under the assumption of $D_s = D_d/10$) were 0.13, 0.91, and 0.84 for phenanthrene, fluoranthene, and pyrene, respectively. Although perhaps indicative of significant DOC-sorbed PAH lability these values should be treated with caution given the uncertainty in D_s. The assumption of a single literature value for D_s is a gross oversimplification since DOC is a dynamic and complex system of aggregates composed of differently sized interacting macromolecules.[38] Therefore, depending on the aqueous environment, and how this affects the DOC aggregation behavior and size, sorption propensity and lability, specific fractions will differently contribute to the observed mass transport. It is recommended that in future experiments of this type, more concerted efforts be directed to obtaining information on the DOC size fractions and their sorption characteristics to further refine the values for D_s. In this way, it will be possible to use experimental data more successfully in conjunction with the existing theory[19,18] to determine, for example, ξ.

Initial PAH Mass Transfer Rates. The magnitude of the rate constants k_d or k_{tot} indicates how fast the system approaches a partitioning equilibrium. Therefore, k_{tot} decreases with increasing DOC concentration and PAH hydrophobicity because an increased mass of compound needs to transfer into the aqueous phase before equilibrium is reached. However, the mass transfer rate $\partial c_{tot}/\partial t$ is given by the product of k_{tot} and the pertaining concentration gradient $(C_{eq,tot} - C_{tot})$. In the field, HOCs entering the aqueous compartment via mass transfer out of the NAPL phase are subject to biodegradation or advective transport. Therefore, the scenario where the aqueous concentrations are kept low, and thus $\partial c_{tot}/\partial t$ is maintained close to its maximum, is particularly relevant in terms of understanding biodegradation or remediation using flushing technologies. Figure 5 compares the initial PAH mass transfer rates for the experiments with saline medium and the two DOC treatments. These were calculated using the fitted values of k_d and $c_{d(eq)}$ or k_{tot} and $c_{tot(eq)}$ (from Tables S7 and S8), and assuming that c_d and c_t in eqs 2 and 4 are zero. These represent the initial (and indeed maximum possible) values of the dissolution rate $\partial c_{tot}/\partial t$. The lower DOC concentration of 0.0226 g L^{-1} had only a minor effect on the initial mass transfer rates, with similar rates being observed in the presence of DOC. However, for the higher DOC concentration of 0.226 g L^{-1} higher initial mass transfer rates were observed for the more hydrophobic PAHs. Relative to the case of saline medium only, initial rates were increased by factors of 1.4, 3.7, and 3.3 for phenanthrene, fluoranthene, and pyrene, respectively. Therefore, high concentrations of DOC increase mass transfer rates of more

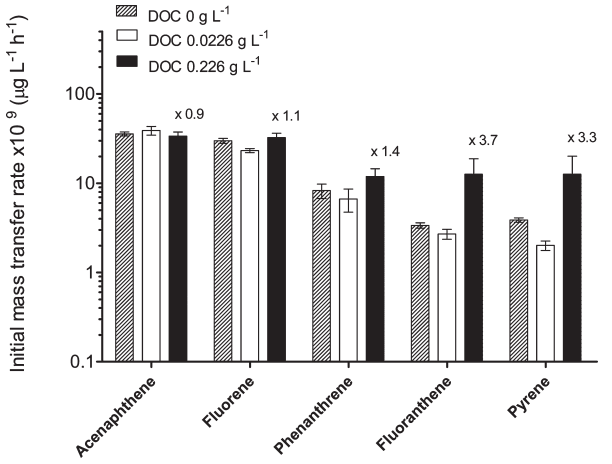

Figure 5. Initial mass transfer rates for DOC concentrations of 0, 0.0226, and 0.226 g L^{-1}. These were calculated using eqs 2 and 4 and setting c_d or c_{tot} to zero. Standard errors were calculated using error propagation. For the DOC 0.226 g L^{-1} concentration, the factor increases in the initial mass transfer rates relative to those measured in the absence of DOC are shown.

hydrophobic NAPL constituents such as PAHs out a NAPL and into the aqueous phase.

Implications for Biodegradation and Toxicity. Figure S9 shows simulated profiles in c_{tot} and c_d for acenaphthene and pyrene as representative low and high hydrophobicity HOCs. When the DOC concentration is sufficiently high and there is significant sorption of the HOC, then DOC increases both the mass transfer rates but also the final amounts in the aqueous compartment. Both dissolved and DOC-sorbed HOCs are accessible to the degradation activities of microorganisms[28,39] and this could lead to increased biodegradation. However, in the case of bioconcentration and toxicity, final levels reached in the organisms are determined by the dissolved concentrations.[8] Despite the increase in HOC masses that are transferred into the aqueous phase with DOC, there is little difference in the time profiles of c_d (Figure S9). Therefore, increased mass transfer rates in the presence of DOC may lead to enhanced biodegradation of NAPL-phase HOCs but have a small influence on their final bioconcentration and toxicity. On the other hand, DOC might enhance bioconcentration and toxicity for mobile organisms with short-time exposure to HOC hotspots.

Relevance of DOC Enhanced Diffusion. The relevance of a DOC-mediated diffusion pathway has to be kept in mind. The lower DOC 0.0226 g L^{-1} concentration is within the range found in marine algal blooms[40] or marine sediment porewaters,[41] and did not significantly enhance $\partial c_{tot}/\partial t$. A measurable increase was only observed at the highest DOC concentration of 0.226 g L^{-1}, and here only for the more hydrophobic PAHs tested in this study. However, such high DOC concentrations are confined to rather specific environments such as wastewater treatment plants or oil-processing waters containing added xanthan gums. Nevertheless, a potential application for DOC-enhanced transfer is in engineered systems where artificially high concentrations can be applied. One example could be using DOC solutions for pump-and-treat NAPL bioremediation technologies, with the low cost and low toxicity of the DOC also being advantageous. The flushing of a soil contaminated with diesel with a 0.8 g L^{-1} humic acid solution increased both the solubilization and biodegradation of naphthalenes leading to shorter remediation times.[42]

Figure S10 shows the calculated enhancement in k_{tot} relative to $k_{tot,dissolved}$ for a series of hypothetical HOCs possessing log $K_{DOC/d}$ values between 1 and 7. These were calculated using the mean k_d, k_d* and k_s*·ξ values measured in this study. Given that the importance of DOC-enhanced diffusion increases with DOC concentration and compound sorption (as indicated by eq 7), for "super" hydrophobic compounds this pathway could both dominate and increase mass transfer rates by orders of magnitude, even at environmental DOC concentrations. Future enhanced diffusion investigations might focus on such compounds, which incidentally are the more difficult compounds to (bio)remediate.

This study was conducted using DOC of terrestrial origin, and the marine backdrop meant the experiments were conducted in a saline aqueous environment. In the wider context of DOC-enhanced diffusion, the relevant properties are reversible sorption of the HOCs and the DOC mobility in the aqueous phase.[17] These apply to other types of DOC in different environments including soils and groundwater, and thus DOC-enhanced diffusion will also likely play a role here. However, to move to the next level of describing DOC-enhanced diffusion in terms of fundamental system and chemical properties will require additional study, with emphasis on the nature of the DOC (size distribution, HOC sorption propensity, sorption/desorption kinetics, lability, etc.) but also for HOCs covering a more diverse range in molecular sizes and structures.

■ ASSOCIATED CONTENT

Ⓢ Supporting Information. Full versions of the materials and methods and modeling description; additional figures and tables showing measurement data from this study. This information is available free of charge via the Internet at http://pubs.acs.org.

■ AUTHOR INFORMATION

Corresponding Author

*Phone: +45 87158463; fax: + 45 46301114; e-mail: kil@dmu.dk.

Present Addresses

†Department of Environmental Science, Faculty of Science and Technology, Aarhus University, Frederiksborgvej 399, 4000 Roskilde, Denmark.

■ ACKNOWLEDGMENT

This work was funded by the European Community Project FACEiT [STREP − Grant 018391 (GOCE)]. Skilled technical help by Birgit Würz and Jana Reichenbach is gratefully acknowledged. The disposable SPME fibers were kindly provided by Philipp Mayer.

■ REFERENCES

(1) Schluep, M.; Gälli, R.; Imboden, D. M.; Zeyer, J. Dynamic equilibrium dissolution of complex nonaqueous phase liquid mixtures into the aqueous phase. *Environ. Toxicol. Chem.* **2002**, *21*, 1350–1358.

(2) Schluep, M.; Imboden, D. M.; Galli, R.; Zeyer, J. Mechanisms affecting the dissolution of nonaqueous phase liquids into the aqueous phase in slow-stirring batch systems. *Environ. Toxicol. Chem.* **2001**, *20*, 459–466.

(3) Ortiz, E.; Kraatz, M.; Luthy, R. G. Organic phase resistance to dissolution of polycyclic aromatic hydrocarbon compounds. *Environ. Sci. Technol.* **1999**, *33*, 235–242.

(4) Wick, L. Y.; Colangelo, T.; Harms, H. Kinetics of mass transfer-limited bacterial growth on solid PAHs. *Environ. Sci. Technol.* **2001**, *35*, 354–361.

(5) van Loosdrecht, M. C. M.; Lyklema, J.; Norde, W.; Zehnder, A. J. B. Influence of interfaces on microbial activity. *Microbiol. Rev.* **1990**, *54*, 75–87.

(6) Bayen, S.; ter Laak, T. L.; Buffle, J.; Hermens, J. L. M. Dynamic exposure of organisms and passive samplers to hydrophobic chemicals. *Environ. Sci. Technol.* **2009**, *43*, 2206–2215.

(7) Stroo, H. F.; Unger, M.; Ward, C. H.; Kavanaugh, M. C.; Vogel, C.; Leeson, A.; Marqusee, J. A.; Smith, B. P. Remediating chlorinated solvent source zones. *Environ. Sci. Technol.* **2003**, *37*, 224A–230A.

(8) Escher, B. I.; Hermens, J. L. M. Internal exposure: Linking bioavailability to effects. *Environ. Sci. Technol.* **2004**, *38*, 455A–462A.

(9) Soga, K.; Page, J. W. E.; Illangasekare, T. H. A review of NAPL source zone remediation efficiency and the mass flux approach. *J. Hazard. Mater.* **2004**, *110*, 13–27.

(10) Pennell, K. D.; Abriola, L. M.; Weber, W. J. Surfactant-enhanced solubilization of residual dodecane in soil columns. 1. Experimental investigation. *Environ. Sci. Technol.* **1993**, *27*, 2332–2340.

(11) Pennell, K. D.; Jin, M. Q.; Abriola, L. M.; Pope, G. A. Surfactant enhanced remediation of soil columns contaminated by residual tetrachloroethylene. *J. Contam. Hydrol.* **1994**, *16*, 35–53.

(12) Ghoshal, S.; Pasion, C.; Alshafie, M. Reduction of benzene and naphthalene mass transfer from crude oils by aging-induced interfacial films. *Environ. Sci. Technol.* **2004**, *38*, 2102–2110.

(13) Johnsen, A. R.; Karlson, U. Evaluation of bacterial strategies to promote the bioavailability of polycyclic aromatic hydrocarbons. *Appl. Microbiol. Biotechnol.* **2004**, *63*, 452–459.

(14) Law, A. M. J.; Aitken, M. D. Bacterial chemotaxis to naphthalene desorbing from a nonaqueous liquid. *Appl. Environ. Microbiol.* **2003**, *69*, 5968–5973.

(15) García-Junco, M.; Gomez-Lahoz, C.; Niqui-Arroyo, J. L.; Ortega-Calvo, J. J. Biosurfactant- and biodegradation-enhanced partitioning of polycyclic aromatic hydrocarbons from nonaqueous-phase liquids. *Environ. Sci. Technol.* **2003**, *37*, 2988–2996.

(16) Mukherji, S.; Weber, W. J. Mass transfer effects on microbial uptake of naphthalene from complex NAPLs (vol 60, pg 750, 1998). *Biotechnol. Bioeng.* **2001**, *75*, 130–141.

(17) Higuchi, W. I. Effects of interacting colloids on transport rates. *J. Pharm. Sci.* **1964**, *53*, 532.

(18) de Jong, H. G.; van Leeuwen, H. P.; Holub, K. Voltammetry of metal-complex systems with different diffusion-coefficients of the species involved. Part i. Analytical approaches to the limiting current for the general-case including association/dissociation kinetics. *J. Electroanal. Chem.* **1987**, *234*, 1–16.

(19) de Jong, H. G.; van Leeuwen, H. P. Voltammetry of metal-complex systems with different diffusion-coefficients of the species involved. Part ii. Behavior of the limiting current and its dependence on association dissociation/kinetics and lability. *J. Electroanal. Chem.* **1987**, *234*, 17–29.

(20) Johnson, J. C.; Sun, S. B.; Jaffe, P. R. Surfactant enhanced perchloroethylene dissolution in porous media: The effect on mass transfer rate coefficients. *Environ. Sci. Technol.* **1999**, *33*, 1286–1292.

(21) Prak, D. J. L.; Abriola, L. M.; Weber, W. J.; Bocskay, K. A.; Pennell, K. D. Solubilization rates of n-alkanes in micellar solutions of nonionic surfactants. *Environ. Sci. Technol.* **2000**, *34*, 476–482.

(22) Mayer, A. S.; Zhong, L. R.; Pope, G. A. Measurement of mass-transfer rates for surfactant-enhanced solubilization of nonaqueous phase liquids. *Environ. Sci. Technol.* **1999**, *33*, 2965–2972.

(23) Benhabib, K.; Town, R. M.; van Leeuwen, H. P. Dynamic speciation analysis of atrazine in aqueous latex nanoparticle dispersions using solid phase microextraction (SPME). *Langmuir* **2009**, *25*, 3381–3386.

(24) ter Laak, T. L.; Van Eijkeren, J. C. H.; Busser, F. J. M.; Van Leeuwen, H. P.; Hermens, J. L. M. Facilitated transport of polychlorinated biphenyls and polybrominated diphenyl ethers by dissolved organic matter. *Environ. Sci. Technol.* **2009**, *43*, 1379–1385.

(25) Mayer, P.; Fernqvist, M. M.; Christensen, P. S.; Karlson, U.; Trapp, S. Enhanced diffusion of polycyclic aromatic hydrocarbons in artificial and natural aqueous solutions. *Environ. Sci. Technol.* **2007**, *41*, 6148–6155.

(26) Kramer, N. I.; van Eijkeren, J. C. H.; Hermens, J. L. M. Influence of albumin on sorption kinetics in solid-phase microextraction: Consequences for chemical analyses and uptake processes. *Anal. Chem.* **2007**, *79*, 6941–6948.

(27) ter Laak, T. L.; ter Bekke, M. A.; Hermens, J. L. M. Dissolved organic matter enhances transport of PAHs to aquatic organisms. *Environ. Sci. Technol.* **2009**, *43*, 7212–7217.

(28) Smith, K. E. C.; Thullner, M.; Wick, L. Y.; Harms, H. Sorption to humic acids enhances polycyclic aromatic hydrocarbon biodegradation. *Environ. Sci. Technol.* **2009**, *43*, 7205–7211.

(29) van Leeuwen, H. P.; Buffle, J. Chemodynamics of aquatic metal complexes: From small ligands to colloids. *Environ. Sci. Technol.* **2009**, *43*, 7175–7183.

(30) Buffle, J.; Wilkinson, K. J.; van Leeuwen, H. P. Chemodynamics and bioavailability in natural waters. *Environ. Sci. Technol.* **2009**, *43*, 7170–7174.

(31) Poerschmann, J.; Zhang, Z.; Kopinke, F.; Pawliszyn, J. Solid phase microextraction for determining the distribution of chemicals in aqueous matrices. *Anal. Chem.* **1997**, *69*, 597–600.

(32) van Leeuwen, H. P. Metal speciation dynamics and bioavailability: Inert and labile complexes. *Environ. Sci. Technol.* **1999**, *33*, 3743–3748.

(33) van Leeuwen, H.; Cleven, R.; Buffle, J. Voltammetric techniques for complexation measurements in natural aquatic media - role of the size of macromolecular ligands and dissociation kinetics of complexes. *Pure Appl. Chem.* **1989**, *61*, 255–274.

(34) Burkhard, L. P. Estimating dissolved organic carbon partition coefficients for nonionic organic chemicals. *Environ. Sci. Technol.* **2000**, *34*, 4663–4668.

(35) Mukherji, S.; Peters, C. A.; Weber, W. J. Mass transfer of polynuclear aromatic hydrocarbons from complex DNAPL mixtures. *Environ. Sci. Technol.* **1997**, *31*, 416–423.

(36) MacKenzie, K.; Georgi, A.; Kumke, M.; Kopinke, F. D. Sorption of pyrene to dissolved humic substances and related model polymers. 2. Solid-phase microextraction (SPME) and fluorescence quenching technique (FQT) as analytical methods. *Environ. Sci. Technol.* **2002**, *36*, 4403–4409.

(37) Pinheiro, J. P.; Mota, A. M.; Goncalves, M. L. S.; van Leeuwen, H. P. The pH effect in the diffusion coefficient of humic matter: Influence in speciation studies using voltammetric techniques. *Colloids Surf., A* **1998**, *137*, 165–170.

(38) Sutton, R.; Sposito, G. Molecular structure in soil humic substances: The new view. *Environ. Sci. Technol.* **2005**, *39*, 9009–9015.

(39) Haftka, J. J. H.; Parsons, J. R.; Govers, H. A. J.; Ortega-Calvo, J. Enhanced kinetics of solid-phase microextraction and biodegradation of polycyclic aromatic hydrocarbons in the presence of dissolved organic matter. *Environ. Toxicol. Chem.* **2008**, *27*, 1526–1532.

(40) Simjouw, J.; Mulholland, M. R.; Minor, E. C. Changes in dissolved organic matter characteristics in Chincoteague Bay during a bloom of the pelagophyte *Aureococcus anophagefferens*. *Estuaries* **2004**, *27*, 986–998.

(41) Deflandre, B.; Gagné, J. Estimation of dissolved organic carbon (DOC) concentrations in nanoliter samples using UV spectroscopy. *Water Res.* **2001**, *35*, 3057–3062.

(42) van Stempvoort, D. R.; Lesage, S.; Novakowski, K. S.; Millar, K.; Brown, S.; Lawrence, J. R. Humic acid enhanced remediation of an emplaced diesel source in groundwater. 1. Laboratory-based pilot scale test. *J. Contam. Hydrol.* **2002**, *54*, 249–276.